Influence of device non-uniformities on the accuracy of Coulomb blockade thermometry

Pekola, Jukka P.

2022-08-01

Pekola , J P , Praks , E , Yurttagül , N & Karimi , B 2022 , ' Influence of device non-uniformities on the accuracy of Coulomb blockade thermometry ' , Metrologia , vol. 59 , no. 4 , 045009 . https://doi.org/10.1088/1681-7575/ac79e8

http://hdl.handle.net/10138/348448
https://doi.org/10.1088/1681-7575/ac79e8

Influence of device non-uniformities on the accuracy of Coulomb blockade thermometry

OPEN ACCESS
IOP Publishing | Bureau International des Poids et Mesures Metrologia
Metrologia **59** (2022) 045009 (8pp) https://doi.org/10.1088/1681-7575/ac79e8

Influence of device non-uniformities on the accuracy of Coulomb blockade thermometry

Jukka P Pekola[1,*], Eemil Praks[1], Nikolai Yurttagül[2] and Bayan Karimi[1,3,*]

[1] Pico Group, QTF Centre of Excellence, Department of Applied Physics, Aalto University School of Science, PO Box 13500, 00076 Aalto, Finland
[2] VTT Technical Research Centre of Finland Ltd, PO Box 1000, FI-02044 VTT Espoo, Finland
[3] QTF Centre of Excellence, Department of Physics, Faculty of Science, University of Helsinki, Finland

E-mail: jukka.pekola@aalto.fi and bayan.karimi@aalto.fi

Received 27 December 2021, revised 14 June 2022
Accepted for publication 17 June 2022
Published 14 July 2022

Abstract
We investigate temperature uncertainty of Coulomb blockade thermometer (CBT) arising from inevitable non-uniformities in tunnel junction arrays. The corrections are proportional to the junction resistance variance in the linear operation regime and this result holds approximately also beyond this originally studied high temperature range. We present both analytical and numerical results, and discuss briefly their implications on achievable uniformity based on state-of-the-art fabrication of sensors.

Keywords: thermometry, Coulomb blockade, non-uniformity errors, low temperature

(Some figures may appear in colour only in the online journal)

1. Introduction

The Coulomb blockade thermometer (CBT) [1] has proven to provide calibration-free thermometry over a wide range from sub-mK up to 70 K [2–7] temperatures T, i.e., over five decades. Its operation is based on bias voltage V dependent conductance G of an array of tunnel junctions under the competition between single-electron charging effects (energy scale E_C) and thermal energy k_BT. The ideal operation range is when $E_C \ll k_BT$; in this linear regime a universal relation [1]

$$V_{1/2} \simeq 5.439 N k_B T/e \tag{1}$$

holds, where $V_{1/2}$ is the full width at half-minimum of the conductance dip around zero bias voltage and N is the number of junctions in series in the array. One may design the thermometer sensor such that the above relation between E_C and k_BT is favorable in the temperature range of interest by engineering the parameters in the array accordingly since E_C, being the charging energy, is inversely proportional to the effective capacitance which is controlled by physical dimensions. Equation (1) is a basis for primary thermometry (calibration-free). When the condition $E_C \ll k_BT$ is compromised, the CBT still yields calibration free thermometry down to much lower temperatures, but with a modified relation between $V_{1/2}$ and T to be discussed below.

Equation (1) and its low temperature versions [10] are strictly valid only for a fully uniform array, where all junction resistances $R_{T,i}$ are equal through the sensor. Figure 1 (top) shows schematically an array of junctions whose sizes vary along the chain. A way of circumventing the issue of non-uniformity induced uncertainty is to measure a single junction embedded in a four probe configuration within junction arrays. This has been analyzed and experimentally demonstrated in [8], and such a configuration provides a partial solution to the problem. In fact it yields a fully accurate thermometer in this respect, but the other side of the coin is that the signal in terms of voltage $V_{1/2}$ is small for such a set-up since $N = 1$ in equation (1). Fortunately the effect of non-uniformity

* Authors to whom any correspondence should be addressed.

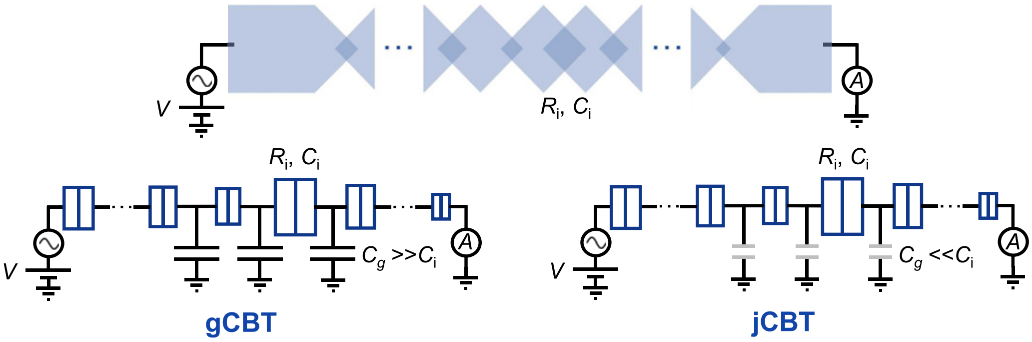

Figure 1. Conceptual illustration of a non-uniform CBT array in the top panel. Two types of CBT are presented in the lower panels where the ground capacitance C_g of each island is either dominating (gCBT on the left) or negligible (jCBT on the right) with respect to junction capacitances C_i.

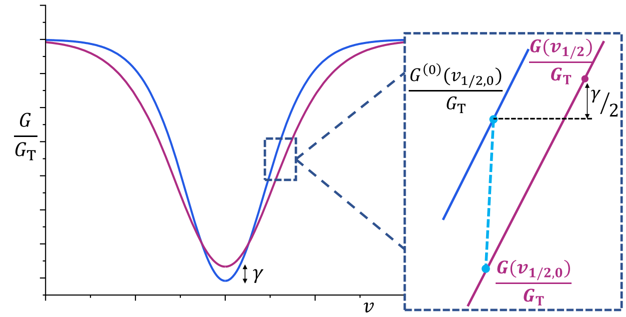

Figure 2. Graphical illustration of how we find correction to half-width for non-uniform arrays and low T corrections. Blue line (deeper and narrower) represents the reference curve and the red one the actual conductance.

is weak in ordinary CBT arrays. However it poses a source of fundamental uncertainty, which is the topic of this article. Some aspects of the problem have been addressed previously in references [9–11]. An experimental investigation of uncertainties in a CBT measurement itself was presented in reference [12].

In this work we present a comprehensive picture of the non-uniformity induced uncertainty in Coulomb blockade thermometry. We discuss two different device classes, (i) the ones where junction resistances vary along the array but capacitance variances are negligible, recently coined gCBT [2], and (ii) those where both resistances and capacitances vary but such that their product remains constant for each element composed of a junction and island between the junctions, jCBT. These two types of CBT are shown schematically in figure 1. Pure capacitance variations with uniform resistances do not lead to temperature corrections in the linear regime, but only to renormalization of charging energy. Devices of type (i) are the ones commonly employed in very low temperature thermometry [2, 3, 13], where self-capacitance of the islands between junctions is intentionally increased to bring E_C down in order to satisfy the conditions discussed above down to low temperatures. On the other hand class (ii) refers to sensors in higher temperature regimes where junction capacitances dominate over self-capacitances of the islands. We take the product of resistance and capacitance to be constant, since the former one is inversely proportional to the overlap area of the junction, whereas the latter one is proportional to it. Naturally analysis is possible also for arrays that are intermediate between these two classes, and their properties can be addressed at least numerically. The general observation is that the non-uniformity induced uncertainty is proportional to the variance of the parameters in all the situations that we consider. Secondly, we find that the analytical results in the linear regime $E_C \ll k_BT$ for the correction in temperature reading stay approximately valid also far beyond this domain, based on our numerical results and an analytic calculation to be presented below. Note that all these results apply also for a CBT sensor consisting of several parallel arrays, as commonly used in the experiments. This is because the uncertainty depends only on the variance of the parameters of the sensor. Another point to note here is that we refer to the low and high temperature regimes meaning either absolute temperature or alternatively that with respect to E_C, depending on the context.

2. Linear regime

We first consider a CBT array of junctions in the linear regime $E_C \ll k_BT$. The conductance G_i of junction i normalized by its inverse tunnel resistance $G_{T,i} = 1/R_{T,i}$ can be written as [8, 9]

$$G_i/G_{T,i} = 1 - \frac{\delta_i}{k_BT} g(v_i), \tag{2}$$

where $v_i = eV_i/k_BT$ is the voltage V_i across junction i in normalized form, δ_i arises from the capacitance matrix of the surrounding circuit (not dependent on resistances of the junctions) and $g(x) = e^x[e^x(x-2)+x+2]/(e^x-1)^3$. Based on current conservation through the array and noting that the bias voltage across the whole array is $V = \sum_i V_i$, we find the normalized conductance of the array, $G(V)$ up to linear order in $(k_BT)^{-1}$ as

$$G(V)/G_T = 1 - \sum_i \frac{R_{T,i}}{R_\Sigma}\frac{\delta_i}{k_BT} g\left(\frac{R_{T,i}}{R_\Sigma}\frac{eV}{k_BT}\right). \tag{3}$$

Here $R_\Sigma = \sum_i R_{T,i} \equiv G_T^{-1}$ is the total resistance of the array. According to this expression, only the resistance non-uniformity affects the absolute temperature reading of the CBT determined by the half-width of the conductance dip, whereas capacitance non-uniformity alone is ineffective.

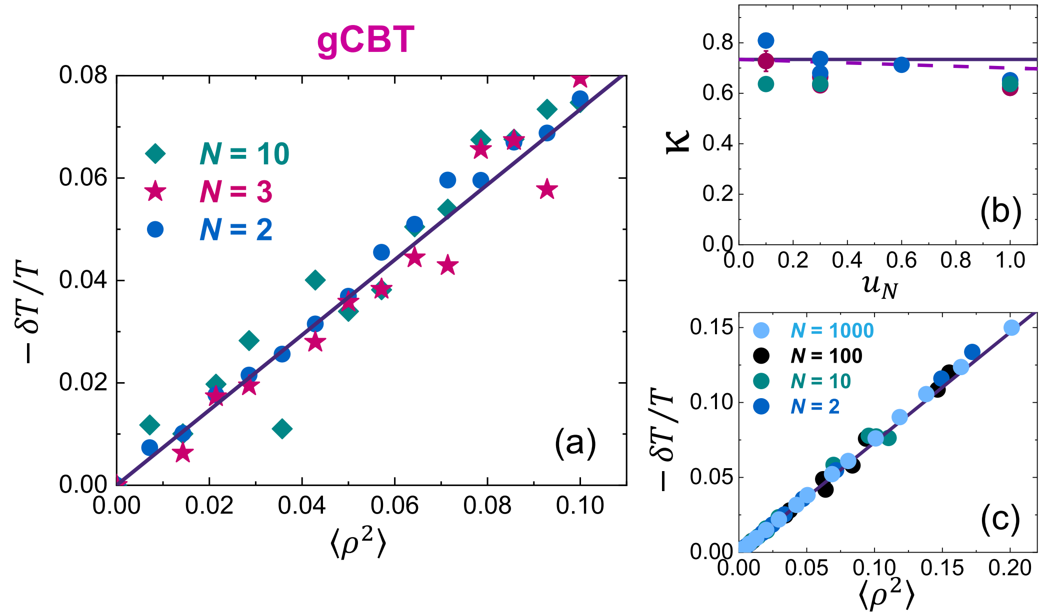

Figure 3. Non-uniformity induced corrections in temperature reading of gCBT. (a) The predicted $-\delta T/T$ vs $\langle\rho^2\rangle$ for three different array lengths N. The solid line is the analytical result of equation (7) valid for all N, and the symbols are calculated numerically with $u_N = 0.3$. (b) The slope $\kappa(-\delta T/T \equiv \kappa\langle\rho^2\rangle)$ of numerically calculated result of (a) as a function of u_N indicating that the $\langle\rho^2\rangle$ dependent correction is close to that in the linear regime (horizontal line) even up to $u_N \sim 1$. The dashed line with a negative slope for $N = 2$ is the result of the analytical calculation from equation (26). (c) Numerical results for non-uniformity induced $-\delta T/T$, based on the universal conductance in the high temperature (linear) approximation, equation (3).

We expand equation (2) up to second order in the relative deviations of junction resistances, $\rho_i = R_{\mathrm{T},i}/R_{\mathrm{ave}} - 1$, where $R_{\mathrm{ave}} = R_\Sigma/N$. We consider two relevant cases (i, gCBT) and (ii, jCBT) described above. Below we normalize all the voltages such that $v = \mathrm{eV}/(Nk_\mathrm{B}T)$ and $v_{1/2} = \mathrm{eV}_{1/2}/(Nk_\mathrm{B}T)$, and denote by $\langle\rho^2\rangle$ the variance of ρ_i.

To obtain the corrections in temperature in general, we can write the following equations linking the actual halfwidth $v_{1/2}$ to $v_{1/2,0} = 2.71959\ldots$, the half-width point of a uniform array from equation (3), i.e. that of the reference curve (see figure 2), as

$$\frac{G(v_{1/2})}{G_\mathrm{T}} = \frac{G^{(0)}(v_{1/2,0})}{G_\mathrm{T}} + \gamma/2$$
$$\frac{G(v_{1/2})}{G_\mathrm{T}} = \frac{G(v_{1/2,0})}{G_\mathrm{T}} + \frac{G'(v_{1/2,0})}{G_\mathrm{T}}(v_{1/2} - v_{1/2,0}). \quad (4)$$

Here γ is the change of the depth of the conductance curve with respect to the reference one with superscript (0) as shown in figure 2. The correction in temperature reading is then $\delta T/T = \delta v_{1/2}/v_{1/2,0}$ where $\delta\, v_{1/2} \equiv v_{1/2} - v_{1/2,0}$. Here and below the measured temperatures based on the half-width of the conductance dip need to be corrected by the factor $(1 + \delta T/T)^{-1}$ to obtain the actual temperature.

(i) gCBT: we find by expanding equation (3) for small $\langle\rho^2\rangle$ that

$$G(v)/G_\mathrm{T} = 1 - u_N g(v) - u_N\left[g'(v)v + \frac{1}{2}g''(v)v^2\right]\langle\rho^2\rangle, \quad (5)$$

where $u_N \equiv \delta_i/k_\mathrm{B}T$ is a constant and prime denotes derivative with respect to v. Using the argument in equation (4) we then find that for the same value of conductance ($\gamma = 0$ here), the bias voltage shifts due to resistance non-uniformity as

$$\delta v_{1/2} = -\left[v_{1/2,0} + \frac{1}{2}\frac{g''(v_{1/2,0})}{g'(v_{1/2,0})}v_{1/2,0}^2\right]\langle\rho^2\rangle. \quad (6)$$

The correction in temperature reading is then

$$\delta T/T \simeq -\left[1 + \frac{1}{2}\frac{g''(v_{1/2,0})}{g'(v_{1/2,0})}v_{1/2,0}\right]\langle\rho^2\rangle \simeq -0.734\,\langle\rho^2\rangle, \quad (7)$$

where the last form arises from $v_{1/2,0} \simeq 2.7196$ in the linear regime, equation (3). Figure 3 presents by solid line the analytical result of equation (7) which is valid for all values of N.

(ii) jCBT: in this case both the width and the depth of the conductance dip are changing. According to [8, 9], we have for the capacitive term in equation (2)

$$\delta_i/e^2 = C^{-1}_{i-1,i-1} + C^{-1}_{i,i} - 2C^{-1}_{i,i-1}. \quad (8)$$

Ignoring the island capacitance fully, the elements on the right-hand side of equation (8) read [15]

$$C^{-1}_{k,l} = \tilde{C}\sum_{m=1}^{\min(k,l)}\frac{1}{C_m}\sum_{\max(k,l)+1}^{N}\frac{1}{C_n}, \quad (9)$$

where C_i is the capacitance of junction i and $\tilde{C}^{-1} = \sum_{k=1}^{N} C_k^{-1}$. If we define C such that $R_{\mathrm{T},i}C_i = R_{\mathrm{ave}}C$, we have $\tilde{C} = C/N$ and

$$\frac{\delta_i}{k_\mathrm{B}T} = \frac{e^2}{k_\mathrm{B}TC}\left[\frac{R_{\mathrm{T},i}}{R_{\mathrm{ave}}} - \left(\frac{R_{\mathrm{T},i}}{R_{\mathrm{ave}}}\right)^2/N\right]. \quad (10)$$

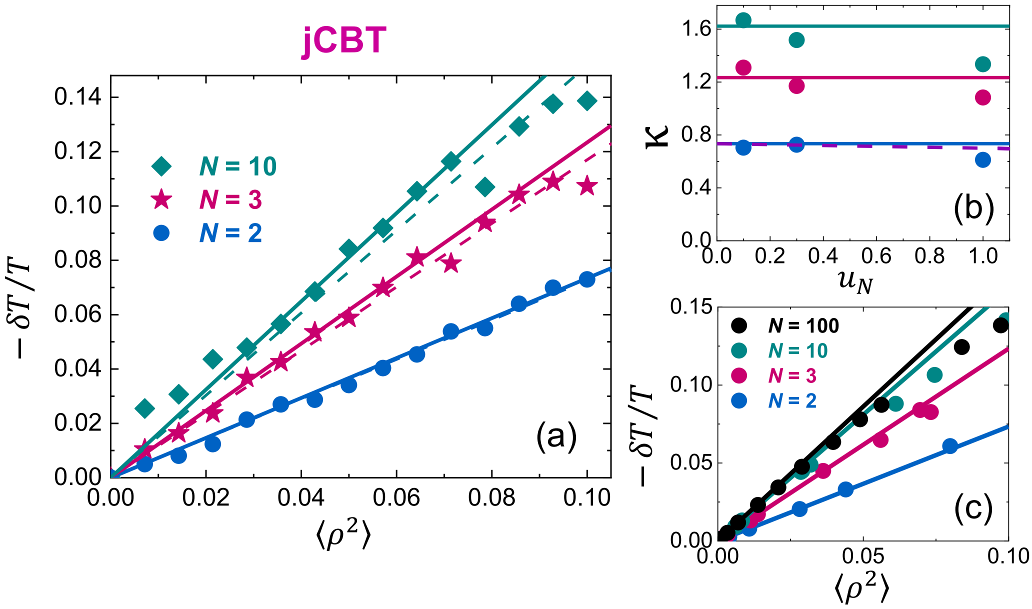

Figure 4. Non-uniformity induced corrections in temperature reading of jCBT. (a) The predicted $-\delta T/T$ vs $\langle\rho^2\rangle$ for three different array lengths N. The solid lines are the analytical results of equation (13), and the symbols are calculated numerically with $u_N = 0.3$. The dashed lines are the linear fits to the latter data. (b) The slope κ, where $-\delta T/T = \kappa\langle\rho^2\rangle$, of numerically calculated results from (a) as a function of u_N indicating that the $\langle\rho^2\rangle$ dependent result is close to that in the linear regime (horizontal lines, $N = 10, 3, 2$ from top to bottom) even up to $u_N \sim 1$. The dashed line with a small negative slope for $N = 2$ is the result of the analytical calculation from equation (26). (c) Numerical results for non-uniformity induced $-\delta T/T$, based on the linear conductance in the high temperature approximation, equation (3).

With similar approximations as above, we find that the zero bias $v = 0$ conductance has the value

$$G(0)/G_\mathrm{T} = 1 - \frac{e^2}{6k_\mathrm{B}TC}\frac{N-1}{N}\left[1 + \frac{N-3}{N-1}\langle\rho^2\rangle\right]. \quad (11)$$

At finite v we have

$$G(v)/G_\mathrm{T} = 1 - \frac{e^2}{k_\mathrm{B}TC}\left\{\frac{N-1}{N}g(v) + \left[\frac{N-3}{N}g(v) + \frac{2N-3}{N}vg'(v) + \frac{N-1}{2N}v^2g''(v)\right]\langle\rho^2\rangle\right\}. \quad (12)$$

Note that $u_N = \frac{e^2\langle 1/C\rangle}{k_\mathrm{B}T}\frac{N-1}{N}$ in this case, where $\langle 1/C\rangle$ is the average of inverse junction capacitances C_i. Again using equation (4) we find

$$\delta T/T \simeq -\left[\frac{2N-3}{N-1} + \frac{1}{2}\frac{g''(v_{1/2,0})}{g'(v_{1/2,0})}v_{1/2,0}\right]\langle\rho^2\rangle$$
$$\simeq -\left[\frac{2N-3}{N-1} - 0.265\,945\right]\langle\rho^2\rangle. \quad (13)$$

Here the last step arises since $\frac{g''(v_{1/2,0})}{2g'(v_{1/2,0})}v_{1/2,0} \simeq -0.265\,945$. Unlike for gCBT in (i), here the correction depends on N. We note that the results of (i) and (ii) are equal for $N = 2$ as they should.

Figure 4 presents by solid lines the analytical results on non-uniformity induced corrections in jCBT for different values of N. Equations (7) and (13) are the main results of the paper in the linear regime.

3. Beyond the linear regime

To obtain the linear in u_N results above, the actual charge distribution on the islands plays no role. This, however, is not the case at low relative temperatures, $k_\mathrm{B}T \lesssim E_\mathrm{C}$. To see how the conductance given by equation (3) gets modified in this case, in particular to find the corresponding expression up to u_N^2, we take the simple two-junction device. In the following we write $u \equiv u_2$ for brevity. First we find the charge distribution, i.e. the occupation probability $\sigma(n)$ for different electron numbers on the island, which is governed by the solution of the master equation

$$\dot{\sigma}(n) = \left[\Gamma_1^+(n-1) + \Gamma_2^-(n-1)\right]\sigma(n-1) + \left[\Gamma_1^-(n+1) + \Gamma_2^+(n+1)\right]\sigma(n+1) - \left[\Gamma_1^+(n) + \Gamma_1^-(n) + \Gamma_2^+(n) + \Gamma_2^-(n)\right]\sigma(n) \quad (14)$$

in steady state $\dot{\sigma}(n) = 0$. Here $\Gamma_i^\pm(m)$ is the tunneling rate in junction $i = 1, 2$ in either forward (+) or backward (−) direction with m extra electrons on the island. The key idea here is to assume that the distribution in the thermometer is broad such that the occupation $\sigma(n)$ is a smooth function of n, extending over many possible values of n such that it can be taken as a continuous variable [10]. In fact the variance of the electron number (at zero bias voltage) is simply $\langle\delta n^2\rangle = 1/u$ thus becoming very wide for $E_\mathrm{C} \ll k_\mathrm{B}T$. Expanding equation (14) in n yields

$$[(\Gamma_2^+(n) - \Gamma_2^-(n)) - (\Gamma_1^+(n) - \Gamma_1^-(n))]\sigma(n) + \frac{\partial}{\partial n}\left\{[\Gamma_1^+(n) + \Gamma_1^-(n) + \Gamma_2^+(n) + \Gamma_2^-(n)]\sigma(n)\right\} = 0. \quad (15)$$

To obtain the rates $\Gamma_i^{\pm}(n)$ we write the energy cost of each event for the system biased at voltage V as $\delta F_i^{\pm} = \pm \mathrm{eV}_i + \delta E_i^{\pm}(n)$, where $V_i = (R_i/R_\Sigma)V$ is the voltage drop across each junction with resistance R_i, and $R_\Sigma = R_1 + R_2$. $\delta E_i^{\pm}(n)$ is the change of the charging energy $E_\mathrm{C} = (ne)^2/(2C_\Sigma)$ ignoring the offset charges (validated by the broad distribution in n). Here $C_\Sigma \equiv C_1 + C_2$. Normalizing the energies as $\delta f_i^{\pm} \equiv \delta F_i^{\pm}/(k_\mathrm{B}T)$, we can write for each event then $\delta f_1^{+}(n) = v_1 + \delta\epsilon_1^{+}$, $\delta f_1^{-}(n) = -v_1 + \delta\epsilon_1^{-}$, $\delta f_2^{+}(n) = v_2 + \delta\epsilon_2^{+}$, $\delta f_2^{-}(n) = -v_2 + \delta\epsilon_2^{-}$, where $v_i = \mathrm{eV}_i/(k_\mathrm{B}T)$, $\delta\epsilon_1^{+} = \delta\epsilon_2^{-} = (1/2+n)u$ and $\delta\epsilon_1^{-} = \delta\epsilon_2^{+} = (1/2-n)u$. The rates themselves are given by the standard expression for normal metal junctions [15] as

$$\Gamma_i^{\pm}(n) = \frac{1}{e^2 R_i} \frac{\delta F_i^{\pm}(n)}{1 - \mathrm{e}^{-\delta F_i^{\pm}(n)/(k_\mathrm{B}T)}}. \quad (16)$$

Our strategy is to expand the rates in powers of u to obtain the results for the thermometer in its working regime $u \lesssim 1$. In the leading order in u we then obtain

$$[\Gamma_2^{+}(n) - \Gamma_2^{-}(n)] - [\Gamma_1^{+}(n) - \Gamma_1^{-}(n)] = \frac{k_\mathrm{B}T}{e^2}\left[\left(\frac{1}{R_1} + \frac{1}{R_2}\right)n - \frac{1}{2}\left(\frac{1}{R_1} - \frac{1}{R_2}\right) + \left(\frac{q(v_1)}{R_1} - \frac{q(v_2)}{R_2}\right)\right]u, \quad (17)$$

where $q(x) = [1-(1+x)e^{-x}]/(1-e^{-x})^2$. Similarly we obtain

$$\Gamma_1^{+}(n) + \Gamma_1^{-}(n) + \Gamma_2^{+}(n) + \Gamma_2^{-}(n) = \frac{k_\mathrm{B}T}{e^2}\left[\frac{h(v_1)}{R_1} + \frac{h(v_2)}{R_2} + \left\{2n\left(\frac{q(v_2)}{R_2} - \frac{q(v_1)}{R_1}\right) + n\left(\frac{1}{R_1} - \frac{1}{R_2}\right) - \frac{1}{2}\left(\frac{1}{R_1} + \frac{1}{R_2}\right)\right\}u\right], \quad (18)$$

where $h(x) \equiv x\coth(x/2)$. Inserting equations (17) and (18) into (15) we obtain

$$u(1/R_1 + 1/R_2)n\sigma(n) + \frac{1}{2}(h(v_1)/R_1 + h(v_2)/R_2)\sigma'(n) = 0. \quad (19)$$

Here we have ignored contributions proportional to $u\delta R$ as small, where $\delta R \equiv (R_1 - R_2)/2$. Equation (19) yields a Gaussian distribution, which by normalization $\int_{-\infty}^{\infty}\sigma(n)\mathrm{d}n = 1$ reads

$$\sigma(n) = \sqrt{\frac{\left(\frac{1}{R_1} + \frac{1}{R_2}\right)u}{\pi\left(\frac{h(v_1)}{R_1} + \frac{h(v_2)}{R_2}\right)}} \exp\left(-\frac{\left(\frac{1}{R_1} + \frac{1}{R_2}\right)u}{\frac{h(v_1)}{R_1} + \frac{h(v_2)}{R_2}}n^2\right). \quad (20)$$

The procedure to obtain the conductance G of the thermometer is to write the current through each junction as

$$I_i(v_i) = e\int[\Gamma_i^{+}(n) - \Gamma_i^{-}(n)]\sigma(n)\mathrm{d}n. \quad (21)$$

The conductance of junction i, G_i, yields the conductance of the thermometer as $G = \mathrm{d}I/\mathrm{d}V = G_1G_2/(G_1+G_2)$. Taking terms up to u^2 we find for junction 1

$$G_1 = \frac{R_2}{R_1+R_2}\left\{1 - ug(v_1) - \frac{u^2}{4}\left[g''(v_1)\left(\frac{h(v_1)}{R_1} + \frac{h(v_2)}{R_2}\right) + g'(v_1)\left(\frac{h'(v_1)+h'(v_2)}{R_1}\right)\right]\right\}, \quad (22)$$

and G_2 can be obtained by permuting the indices 1 and 2. We then finally have up to u^2

$$\begin{aligned} G(v)/G_\mathrm{T} = 1 - ug(v) - \frac{u^2}{4}[g'(v)h'(v) + g''(v)h(v)] \\ - \left\{u\left[vg'(v) + \frac{1}{2}v^2g''(v)\right] + \frac{u^2}{4}\left[4v^2g'(v)^2\right.\right. \\ - g'(v)h'(v) + vg'''(v)h(v) - vg''(v)h'(v) \\ + \frac{1}{2}v^2g''''(v)h(v) + \frac{1}{2}v^2g'''(v)h'(v) \\ \left.\left. + \frac{1}{2}v^2g''(v)h''(v) + \frac{1}{2}v^2g'(v)h'''(v)\right]\right\}\langle\rho^2\rangle. \end{aligned} \quad (23)$$

In the next sections we use the result of equation (23) with two different aims: to evaluate the second order corrections to the conductance curve and its width for both uniform [10] and non-uniform CBT.

3.1. Correction to halfwidth in a uniform array due to non-vanishing u

Here we investigate the uniform array within the second order approximation of equation (23). Then the lengthy contribution proportional to $\langle\rho^2\rangle$ vanishes, and we have

$$G(v)/G_\mathrm{T} = G^{(0)}(v)/G_\mathrm{T} - \frac{u^2}{4}[g'(v)h'(v) + g''(v)h(v)], \quad (24)$$

where $G^{(0)}(v)/G_\mathrm{T} \equiv 1 - ug(v)$ yields the standard halfwidth $v_{1/2,0}$ for a vanishingly small u. Equation (24) is valid for general N when replacing u by u_N [10].

The known [10] lowest order correction to $v_{1/2,0}$ of a uniform CBT due to non-vanishing u can again be obtained with the help of equation (4) and figure 2. Including the second order correction to G in equation (24) suppresses partly the depth of the dip $\Delta G/G_\mathrm{T}$ from $u/6$ to $u/6 - u^2/60$, i.e. $\gamma = u^2/60$. Up to linear order in u we can then write the solution as

$$\begin{aligned} \frac{\delta T}{T} &= \frac{v_{1/2}}{v_{1/2,0}} - 1 \\ &= -\frac{1 + 30[g'(v_{1/2,0})h'(v_{1/2,0}) + g''(v_{1/2,0})h(v_{1/2,0})]}{20g'(v_{1/2,0})v_{1/2,0}} \\ &\quad \times \frac{\Delta G}{G_\mathrm{T}} \simeq 0.3921\frac{\Delta G}{G_\mathrm{T}}, \end{aligned} \quad (25)$$

where $\Delta G/G_\mathrm{T}$ is the measured depth of the dip.

Table 1. Summary of the main results governing CBT in different regimes.

	Conductance	Temperature
Uniform array, linear regime ($E_C \ll k_B T$)	$G/G_T = 1 - u_N g(v)$	$T = 0.183\,85 \frac{eV_{1/2}}{N k_B}$
Non-uniform array, linear regime	$G/G_T = 1 - \sum_i \frac{R_{T,i}}{R_\Sigma} \frac{\delta_i}{k_B T} g(\frac{R_{T,i}}{R_\Sigma} \frac{eV}{k_B T})$	$\delta T/T \simeq -0.734\langle\rho^2\rangle$ (gCBT) $\delta T/T \simeq -\left[\frac{2N-3}{N-1} - 0.265\,945\right]\langle\rho^2\rangle$ (jCBT)
Uniform array, beyond linear regime	$G/G_T = 1 - u_N g(v) - \frac{u_N^2}{4}[g'(v)h'(v) + g''(v)h(v)]$	$\delta T/T \simeq 0.3921 \frac{\Delta G}{G_T}$
Non-uniform array, beyond linear regime $N = 2$	Equation (23)	$\frac{\delta T}{T} = 0.3921\frac{\Delta G}{G_T} - (0.734 - 0.205\frac{\Delta G}{G_T})\langle\rho^2\rangle$

3.2. Correction to halfwidth from non-uniformities for non-vanishing u

We consider for simplicity the case $N = 2$ and use again equation (4) to obtain the uncertainty in temperature reading via deformation of the G/G_T vs v analytically. If we write equation (23) in the form $G/G_T = 1 - ug(v) + u^2 L(v) + [uJ(v) + u^2 B(v)]\langle\rho^2\rangle$ with obvious notations for L, J and B we find the temperature uncertainty arising from the non-uniformity in this case as

$$\delta T/T = -\frac{J(v_{1/2}) + uB(v_{1/2})}{v_{1/2}[g'(v_{1/2}) + uL'(v_{1/2})]}\langle\rho^2\rangle. \qquad (26)$$

Up to linear order in u, the non-uniformity induced uncertainty is $\delta T/T = -(0.734 - 0.0341u)\langle\rho^2\rangle$.

4. Summary of the analytic temperature corrections of CBT

Equations (25) and (26) yield the analytical expression of how the temperature depends on both $\langle\rho^2\rangle$ and u up to linear order in $\Delta G/G_T \simeq u/6$ given by

$$\frac{\delta T}{T} = 0.3921\frac{\Delta G}{G_T} - \left(0.734 - 0.205\frac{\Delta G}{G_T}\right)\langle\rho^2\rangle. \qquad (27)$$

The two contributions have naturally a fully different position as corrections [16]. The first part of this, $0.3921\Delta G/G_T$, given by equation (25) is common for both gCBT and jCBT. One can naturally take into account and correct by measuring the $\Delta G/G_T$. On the contrary, the second part proportional to $\langle\rho^2\rangle$ remains as uncertainty that is difficult to correct for, and it depends on the fabrication uniformity of the CBT sensors. Measurements of this type of sensors [17] show that resistance uniformities below 5% are achievable, which corresponds to $\langle\rho^2\rangle \leqslant 0.0025$. Equation (27) is fully valid for $N = 2$ only, whereas the coefficients 0.3921 and 0.734 apply for general N in gCBT.

It is worth noting that the non-uniformity of gCBT does not lead to corrections in the depth of the zero bias peak. This is seen for instance by setting $v = 0$ in equation (23): all the corrections $\propto \langle\rho^2\rangle$ vanish then; this may be a helpful result when using the secondary mode of CBT, i.e. when measuring the depth $\Delta G/G_T$ for thermometry.

The main expressions for corrections and uncertainties in different regimes are summarized in table 1.

5. Validation of the analytical results with numerical simulations

The main features of numerical Monte Carlo simulation for single-electron tunneling are described in [18–20]. Solving island potentials and potential differences between islands is done somewhat differently from what is presented in reference [19]. We assume that one end of the N-junction array is at the ground potential and the other one at potential V. Let $\boldsymbol{\varphi} = \begin{bmatrix}\varphi_1 & \varphi_2 & \dots & \varphi_{n-1}\end{bmatrix}^T$ denote the potential of each island and $\tilde{\boldsymbol{\varphi}} = \begin{bmatrix}\tilde{\varphi}_1 & \tilde{\varphi}_2 & \dots & \tilde{\varphi}_n\end{bmatrix}^T$ is the vector of the voltage across each junction. We have then $V = \sum_{i=1}^n \tilde{\varphi}_i$ and $\tilde{\varphi}_i = \varphi_i - \varphi_{i+1}$. Ignoring the offset charges, which is validated in the range $u_N < 1.5$ [14], these relations can be expressed as a matrix equation $\mathbf{C}\cdot\begin{bmatrix}\tilde{\boldsymbol{\varphi}} \\ \boldsymbol{\varphi}\end{bmatrix} = \begin{bmatrix}V & \boldsymbol{q} & 0 & \dots & 0\end{bmatrix}^T$, where

$$\mathbf{C} = \begin{bmatrix} 1 & 1 & \dots & \dots & 1 & & & \\ C_1 & -C_2 & 0 & & & C_g & & \\ & \ddots & \ddots & \ddots & & & \ddots & \\ & & C_{n-1} & -C_n & 0 & & & C_g \\ & 1 & & 0 & -1 & 1 & & \\ & & \ddots & & \ddots & \ddots & \ddots & \\ & & & \ddots & & \ddots & \ddots & 1 \\ & & & & 1 & & 0 & -1 \end{bmatrix}. \qquad (28)$$

The vector of island charges is $\boldsymbol{q} = \begin{bmatrix}q_1 & q_2 & \dots & q_{n-1}\end{bmatrix}^T$. This procedure allows one to find the island potentials φ_i. The rest of the simulation is similar to that in [19], determining conductance from current.

Figures 3 and 4 present in (a) and (b) results on Monte-Carlo simulations addressing $\langle\rho^2\rangle$ and u_N (i.e. $\Delta G/G_T$) dependence of $-\delta T/T$, together with analytic results. In general one can say that the lowest order results presented in equations (7) and (13) are in practise sufficient to address the corrections of gCBT and jCBT, respectively, up to $u_N \sim 1$. The (c) panels in these figures are from the linear approximation of equation (3) but with randomly generated ensemble of junction non-uniformity with given variation.

Since we are looking for small deviations in the conductance curves, one needs to average the simulated measurement of current versus voltage over a sufficiently long time. This is particularly important for small values of E_C/k_BT, where the zero-bias drop of conductance is small. Typically this means that one needs to simulate $n = 10^9$–10^{10} tunneling events to obtain sufficiently low statistical uncertainty in the data of figures 3 and 4. If one wants to convert this to what it would mean in real measurement time in experiment, one first observes that in the CBT regime each tunneling occurs in an average time of $\sim e^2R_i/k_BT$; therefore the total time that such a simulation corresponds to is $t \sim ne^2R_i/k_BT$. One can see that for $R_i \sim 10$ kΩ and $T \sim 0.1$ K, this would then correspond to seconds of measuring time. Yet even with fast hardware the simulation of such a large number of tunneling events takes tens of hours. Therefore, these calculations are not feasible without sufficient parallelization. In our case the simulations were realized by Aalto University School of Science 'Science-IT' computer resources, allowing for approximately 1000 simulations running in parallel. Still the scatter of the numerical data in figures 3 and 4 is due to the finite computing resource.

6. Discussion

The results presented in this paper are useful for assessing uncertainty in Coulomb blockade thermometry both at very low temperatures, down to sub-mK regime as well as at high temperatures approaching the ambient. In the first case, low T, we observe that the concept of gCBT works generally, and the corrections arise only from the resistance non-uniformity. Furthermore, since the structures are physically large for low temperature CBTs (lower E_C), the variance $\langle\rho^2\rangle$ is also quite small due to smaller relative variations in junction sizes. It is in place to observe that 1% rms-variation in R_i leads to $<10^{-4}$ uncertainty only. On the other hand, the sensors in higher temperature range belong rather to jCBT category where the dominant capacitance is that of the junctions. The higher the temperature, the smaller the junctions are in pursuit of maximum E_C. This is because for practical purposes the depth of the conductance dip $\Delta G/G_T \propto E_C/k_BT$ needs to be of the order of 10^{-2} or greater, otherwise the signal-to-noise ratio would be compromised. Small average junction size leads to inevitable variation in these sizes and thus to increased $\langle\rho^2\rangle$. Yet for practical purposes it is good to keep in mind that a rms-variation of $\sqrt{\langle\rho^2\rangle} = 10\%$ of junctions leads to uncertainty of only less than 2% for any length of the array. Finally this paper extended the nonuniformity analysis beyond the linear $E_C \ll k_BT$ regime. In particular we made the observation that the temperature uncertainty does not change significantly when leaving this regime; this conclusion was based on both numerical Monte-Carlo simulations for arbitrary arrays and on analytical results for $N = 2$. We presented a systematic analysis of corrections in both gCBT and jCBT configurations. Moreover, we analyzed corrections beyond the linear regime for the first time.

Acknowledgement

We thank Joonas T Peltonen for useful discussions. This work was supported by Academy of Finland Grant 312057 (QTF Centre of Excellence), European Microkelvin Platform (EMP, No. 824109 EU Horizon 2020) and Real-K Project (Grant No. 18SIB02). Real-K received funding from the European Metrology Programme for Innovation and Research (EMPIR) co-financed by the Participating States and from the European Union's Horizon 2020 research and innovation programme. The numerical calculations were performed using the computer infrastructure within the Aalto University School of Science (Science-IT).

ORCID iDs

Jukka P Pekola https://orcid.org/0000-0003-0984-1829
Bayan Karimi https://orcid.org/0000-0003-4752-4277

References

[1] Pekola J P, Hirvi K P, Kauppinen J P and Paalanen M A 1994 Thermometry by arrays of tunnel junctions *Phys. Rev. Lett.* **73** 2903

[2] Samani M *et al* Microkelvin electronics on a pulse-tube cryostat with a gate Coulomb blockade thermometer (arXiv:2110.06293)

[3] Sarsby M, Yurttagül N and Geresdi A 2020 500 microkelvin nanoelectronics *Nat. Commun.* **11** 1492

[4] Meschke M, Kemppinen A and Pekola J P 2016 Accurate Coulomb blockade thermometry up to 60 Kelvin *Phil. Trans. R. Soc.* A **374** 20150052

[5] Bradley D I *et al* 2016 Nanoelectronic primary thermometry below 4 mK *Nat. Commun.* **7** 10455

[6] Bradley D I *et al* 2017 On-chip magnetic cooling of a nanoelectronic device *Sci. Rep.* **7** 45566

[7] Palma M, Scheller C P, Maradan D, Feshchenko A V, Meschke M and Zumbühl D M 2017 On-and-off chip cooling of a Coulomb blockade thermometer down to 2.8 mK *Appl. Phys. Lett.* **111** 253105

[8] Pekola J P, Holmqvist T and Meschke M 2008 Primary tunnel junction thermometry *Phys. Rev. Lett.* **101** 206801

[9] Hirvi K P, Kauppinen J P, Korotkov A N, Paalanen M A and Pekola J P 1995 Arrays of normal metal tunnel junctions in weak Coulomb blockade regime *Appl. Phys. Lett.* **67** 2096

[10] Farhangfar S, Hirvi K P, Kauppinen J P, Pekola J P, Toppari J J, Averin D V and Korotkov A N 1997 One dimensional arrays and solitary tunnel junctions in the weak Coulomb blockade regime: CBT thermometry *J. Low Temp. Phys.* **108** 191

[11] Yurttagül N, Sarsby M and Geresdi A 2021 Coulomb blockade thermometry beyond the universal regime *J. Low Temp. Phys.* **204** 143

[12] Hahtela O, Mykkänen E, Kemppinen A, Meschke M, Prunnila M, Gunnarsson D, Roschier L, Penttilä J and Pekola J

2017 Traceable Coulomb blockade thermometry *Metrologia* **54** 69

[13] Jones A T, Scheller C P, Prance J R, Kalyoncu Y B, Zumbühl D M and Haley R P 2020 Progress in cooling nanoelectronic devices to ultra-low temperatures *J. Low Temp. Phys.* **201** 772

[14] Hirvi K P, Paalanen M A and Pekola J P 1996 Numerical investigation of one-dimensional tunnel junction arrays at temperatures above the Coulomb blockade regime *J. Appl. Phys.* **80** 256

[15] Ingold G-L and Nazarov Y V 1992 *Single Charge Tunneling,* ed H Grabert and M H Devoret vol 294 (New York: Plenum Press), p 21

[16] Working Group 1 of the Joint Committee for Guides in Metrology (JCGM/WG 1) 2008 *Metrology, JCGM 100:2008 (GUM 1995 with minor corrections - BIPM)* (https://www.bipm.org/documents/20126/2071204/JCGM_100_2008_E.pdf/cb0ef43f-baa5-11cf-3f85-4dcd86f77bd6)

[17] Peltonen J T and Wang L 2022 Aalto University (unpublished)

[18] Bakhvalov N S, Kazacha G S, Likharev K K and Serdyukova S I 1989 *Sov. Phys - JETP* **68** 581 http://jetp.ras.ru/cgi-bin/dn/e_068_03_0581.pdf

[19] Yurttagül N 2020 *Microkelvin Nanoelectronics: Dissertation* (Gildeprint, Enschede: Delft Technical University) p 177

[20] Wasshuber C 2001 *Computational Single: Electronics,* ed S Selberherr (Berlin: Springer)